Equilibrium distributions in thermodynamical traffic gas

Milan Krbálek
Faculty of Nuclear Sciences and Physical Engineering,
Czech Technical University,
Trojanova 13, 120 00 Prague, Czech Republic

February 6, 2008

Abstract

We derive the exact formula for thermal-equilibrium spacing distribution of one-dimensional particle gas with repulsive potential $V(r) = r^{-\alpha}$ $(\alpha > 0)$ depending on the distance r between the neighboring particles. The calculated distribution (for $\alpha = 1$) is successfully compared with the highway-traffic clearance distributions, which provides a detailed view of changes in microscopical structure of traffic sample depending on traffic density. In addition to that, the observed correspondence is a strong support of studies applying the equilibrium statistical physics to traffic modelling.

PACS numbers: 05.70-a, 05.20-y, 45.70 Vn
Key words: vehicular traffic, one-dimensional gas, power-law interaction potential, spacing distribution

Investigation of one-dimensional particle ensembles seems actually to be very useful for understanding of the complex system called *vehicular traffic*. Beside the favorite cellular automata, in the recent time new trend appears in the traffic modelling. Application of the equilibrium statistical-physics to traffic ensembles (queuing systems of spatially interacting particles) has been more times discussed (see for example Ref. [2] and other references in) and successfully demonstrated in the articles [5], [9], and [7]. It has been manifested in Ref. [9] that thermodynamics approach can be applied to such a many-particle driven system as traffic flow, based on a microscopic description, in analogy to equilibrium physical systems. Besides, it has been demonstrated in Ref. [7] that the relevant statistical distributions obtained from the local thermodynamical model are in accord with those from traffic data measured on real freeways by the induction-loop detectors. It opens up an opportunity for finding the analytical form of probability density for clear distance among the cars (i.e. *clearance distribution* in traffic terminology) moving in traffic stream. Up to the present time the question about analytical form of clearance distribution has only been a subject of speculations (see the Ref. [6], [2]) – never successfully answered.

We aim to use one-dimensional thermodynamical particle gas to the prediction of microscopical structure in traffic flows and consequently make a comparison to the relevant traffic data distributions. Justification for the approach described can be found in Ref. [5] and [3] where it is proved that equilibrium solution of certain family of the particle gases (exposed to the heat bath with the temperature $T \geq 0$) is a good approximation for steady-state solution of driven many-particle systems with asymmetrical interactions. Since the vehicular traffic is a dissipative system of active elements (moving far from equilibrium), it is evident (see Ref. [9] and [5]) that thermodynamics-balance approach can be used on a mesoscopic level only (i.e. for small-sized samples of N vehicles), where the traffic density fluctuates around the constant value and distances and velocities are mutually uncorrelated. Then the stationary solution of relevant Fokker-Planck equation practically coincides with thermal-balance probability density of certain statistical gas (see Ref. [5]). Moreover, the possibility for using the thermodynamical approach is supported by the fact that distribution of velocities in traffic sample fully corresponds to the Gaussian distribution (in each traffic-density interval) – see Ref. [2], [4], and [7]. Overall, it is sufficiently justified that traffic systems can be *locally* (i.e. on a mesoscopic level) described by instruments of equilibrium statistical physics.

Thus, consider N identical particles (vehicles) on the circle of the circumference $L = N$. Let x_i $(i = 1 \ldots N)$ denote the circular position of the ith particle. Put $x_{N+1} = x_1 + 2\pi$, for convenience. Now we introduce the short-ranged potential energy

$$U \propto \sum_{i=1}^{N} V(r_i),$$

where $V(r_i)$ corresponds to the repulsive two-body potential depending on the distance $r_i = |x_{i+1} - x_i| \frac{N}{2\pi}$ between the neighboring particles only. Nearest-neighbor interaction is chosen with the respect to the realistic behavior of car-driver in traffic sample (see Ref. [7]). Besides, the potential $V(r)$ has to be defined so that $\lim_{r \to 0_+} V(r) = \infty$ which prevents particles passing through each other. The

hamiltonian of the described ensemble reads as

$$\mathcal{H} = \frac{1}{2}\sum_{i=1}^{N}(v_i - \overline{v})^2 + C\sum_{i=1}^{N} V(r_i),$$

with the ith particle velocity v_i and the positive constant C. Note that $\overline{v}$ represents the mean velocity in the ensemble. Then, the appropriate partition function[1]

$$\mathcal{Z} = \int_{\mathbb{R}^{2N}} \delta\left(L - \sum_{i=1}^{N} r_i\right) \prod_{i=1}^{N} e^{-\frac{(v_i-\overline{v})^2}{2\sigma^2}}\; e^{-C\frac{V(r_i)}{\sigma^2}} dr_i dv_i \tag{1}$$

leads us (after $2N-1$ integrations) to the simple assertion that velocity v of particles is Gaussian distributed, i.e.

$$P(v) = \frac{1}{\sqrt{2\pi}\sigma}\; e^{-\frac{(v-\overline{v})^2}{2\sigma^2}}$$

is the corresponding probability density.

Of larger interest, however, is the spacing distribution $P_\beta(r)$. To calculate the exact form of $P_\beta(r)$ one can restrict the partition function (1) by N velocity-integrations to the reduced form

$$\mathcal{Z}_N(L) = \int_{\mathbb{R}^N} \delta\left(L - \sum_{i=1}^{N} r_i\right) e^{-\beta\sum_{i=1}^{N} V(r_i)}\, dr_1 \ldots dr_N$$

where $\beta = C\sigma^{-2}$ is *the inverse temperature* (dimensionless) of the heat bath. Denoting $f(r) = e^{-\beta V(r)}$ the previous expression changes to

$$\mathcal{Z}_N(L) = \int_{\mathbb{R}^N} \delta\left(L - \sum_{i=1}^{N} r_i\right) \prod_{i=1}^{N} f(r_i)\, dr_1 \ldots dr_N.$$

Applying the Laplace transformation (see the Ref. [1] for details) one can obtain

$$g_N(p) \equiv \int_0^\infty \mathcal{Z}_N(L)\, e^{-pL}\, dL =$$

$$= \left(\int_0^\infty f(r)e^{-pr}\, dr\right)^N \equiv [g(p)]^N.$$

Then the partition function (in the large N limit) can be computed with the help of Laplace inversion

$$\mathcal{Z}_N(L) = \frac{1}{2\pi\mathtt{i}} \int_{B-\mathtt{i}\infty}^{B+\mathtt{i}\infty} g_N(p)\, e^{Lp}\, dp.$$

Its value is well estimated by the approximation in the saddle point B which is determined using the equation

$$\frac{1}{g(B)}\frac{\partial g}{\partial p}(B) = -\frac{L}{N}.$$

Thus,

$$\mathcal{Z}_N(L) \approx [g(B)]^N\, e^{LB}. \tag{2}$$

[1] σ is the constant representing a statistical variance

Hence the probability density for spacing r_1 between the particles 1 and 2 can be then reduced to the form

$$P(r_1) = \frac{\mathcal{Z}_{N-1}(L-r_1)}{\mathcal{Z}_N(L)} f(r_1).$$

Supposing $N \gg 1$ and using equation (2) we obtain

$$P(r_1) = \frac{1}{g(B)}\, f(r_1)\, e^{-Br_1},$$

which leads (after applying the same procedure for every pair of successive particles) to the distribution function for spacing r between arbitrary couple of neighboring particles

$$P_\beta(r) = A\, e^{-\beta V(r)}\, e^{-Br} \qquad (r \geq 0). \tag{3}$$

Note that constant A assures the normalization $\int_0^\infty P_\beta(r)\; dr = 1$. Furthermore, returning to the original choice $L = N$, the mean spacing is

$$\langle r\rangle \equiv \int_0^\infty rP_\beta(r)\, dr = 1. \tag{4}$$

Two above conditions can be understood as equation system for unknown normalization constants A, B.

Let us to proceed to the special variants of the gas studied. Firstly, we draw our attention to the Coulomb gas with the logarithmic potential

$$V(r) := -\ln(r) \qquad (r > 0).$$

Such a gas (usually called Dyson's gas, for example in Ref. [11]) is frequently used in the many branches of physics (including the traffic research in Ref. [8]) and the corresponding spacing distribution reads as (see Ref. [1])

$$P_\beta(r) = \frac{(\beta+1)^{\beta+1}}{\Gamma(\beta+1)}\, r^\beta e^{-(\beta+1)r},$$

where $\Gamma(\xi)$ is gamma function. Of larger physical interest, as demonstrated in Ref. [5] and [7], seem actually to be the potentials

$$V_\alpha(r) := r^{-\alpha} \qquad (r > 0),$$

for $\alpha > 0$. The aim of the following computational procedure is to normalize the distribution

$$P_\beta(r) = Ae^{-\frac{\beta}{r^\alpha}}e^{-Br}. \tag{5}$$

Consider now the favorable choice $\alpha = 1$, for which the normalization integrals are exactly expressed as

$$\int_0^\infty e^{-\frac{\beta}{r}}e^{-Br}\, dr = 2\sqrt{\frac{\beta}{B}}\, \mathcal{K}_1\left(2\sqrt{\beta B}\right) \tag{6}$$

$$\int_0^\infty re^{-\frac{\beta}{r}}e^{-Br}\, dr = 2\frac{\beta}{B}\, \mathcal{K}_2\left(2\sqrt{\beta B}\right), \tag{7}$$

where $\mathcal{K}_\lambda$ is the Mac-Donald's function (modified Bessel's function of the second kind) of order λ, having for $\lambda = 1$ and $\lambda = 2$ an approximate expression

$$\mathcal{K}_\lambda(y) = \sqrt{\frac{\pi}{2}}e^{-y}\left(y^{-1/2} + \frac{3}{8}5^{\lambda-1}y^{-3/2} + \mathcal{O}\left(y^{-5/2}\right)\right).$$

Applying the equations (6) and (7) to the normalization integrals one can determine the exact values of the constants A and B. Both of them can be, after applying Taylor's expansion procedure, very well estimated by the approximations

$$B \approx \beta + \frac{3 - e^{-\sqrt{\beta}}}{2}, \tag{8}$$

and

$$A \approx \frac{\sqrt{2\beta + 3 - e^{-\sqrt{\beta}}}}{\sqrt{8\beta}\,\mathcal{K}_1\left(\sqrt{4\beta^2 + 6\beta - 2\beta e^{-\sqrt{\beta}}}\right)}. \tag{9}$$

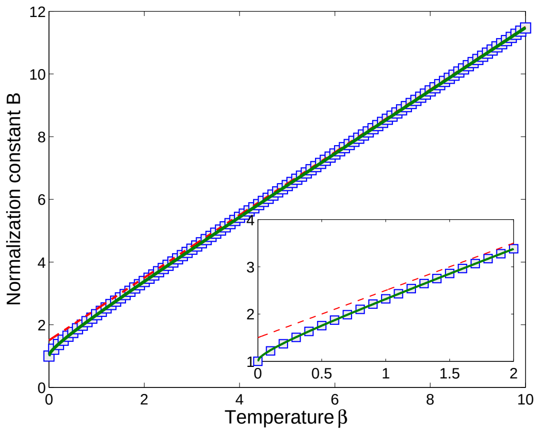

Figure 1. Normalization constant B depending on the inverse temperature β.
Squares represent the exact value of B obtained from numerical computations. The dashed and solid curves display the large β approximation (10) and full approximation (8), respectively. The behavior close to the origin is magnified on the inset.

Finally, we investigate the distribution (5) for general $\alpha > 0$. Although in this case the normalization integrals are not trivially solvable, the scaling (4) leads us to the simple approximate formula

$$B \approx \alpha\beta + 1 + \frac{\alpha}{2} \qquad (\beta \gg 1)\,. \tag{10}$$

The large β estimation $r^{-\alpha} \approx 1 - \alpha + \alpha r^{-1}$, which holds true for values r around mean distance $r \approx 1$, provides the asymptotical formula for normalization constant A :

$$A \approx \frac{1}{2}\sqrt{1 + \frac{1}{2\beta} + \frac{1}{\alpha\beta}}\,\frac{e^{\beta(1-\alpha)}}{\mathcal{K}_1\left(\sqrt{2\alpha\beta(2\alpha\beta + \alpha + 2)}\right)}. \tag{11}$$

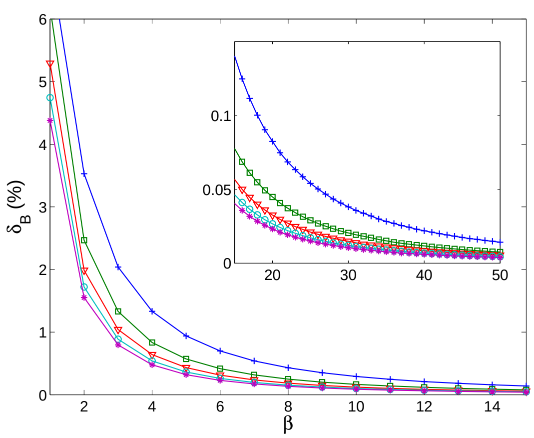

Figure 2. Relative deviation in the approximate value of the normalization constant B as function of parameter β.
We display the deviation (13) between the numerical value B_{ex} and the value B_{est} obtained from the large β approximation (10). The plus signs, squares, triangles, circles and stars correspond to the parameters $\alpha = 1, 2, 3, 4, 5$, respectively. The tails of the curves are magnified on the inset.

For practical applications it seems to be useful to detect the critical inverse temperature β_{crit} under which the relative deviation between the exact (ex) and estimated (est) values of the constant A (or B)

$$\delta_{\log(A)} := \frac{|\log(A_{ex}) - \log(A_{est})|}{\log(A_{ex})} \tag{12}$$

$$\delta_B := \frac{|B_{ex} - B_{est}|}{B_{ex}} \tag{13}$$

are larger then the fixed acceptable deviation δ. For these purposes we plot the functional dependence $\delta_B = \delta_B(\beta)$ and $\delta_{\log(A)} = \delta_{\log(A)}(\beta)$ in the Fig. 2 and Fig. 3, respectively. We note that the exact values A_{ex}, B_{ex} were determined with the help of the numerical computations.

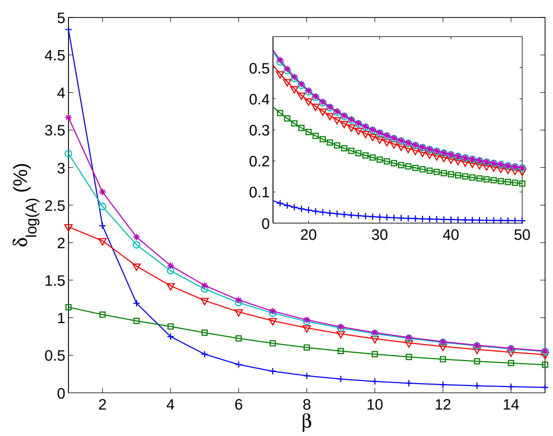

Figure 3. Relative deviation in the approximate value of the normalization constant A as function of parameter β.
Plotted is the deviation (12) between the numerically computed value A_{ex} and the estimated value (11). The symbols used here are consistent with the symbols in the Fig. 2.

Considering now the tested choice for car-car potential $V(r) = r^{-1}$ we intend to compare the equilibrium distribution

$$P_\beta(r) = Ae^{-\frac{\beta}{r}}e^{-Br} \tag{14}$$

with the relevant distributions of single-vehicle data measured continuously during approximately 140 days on the Dutch two-lane freeway A9. Macroscopic traffic density ϱ was calculated for samples of $N = 50$ subsequent cars passing a detector. For the purposes described above we divide the region of the measured densities $\varrho \in [0, 85\ \mathrm{veh/km/lane}]$ into 85 equidistant subintervals and separately analyze the data from each one of them. The sketched procedure prevents the undesired mixing of the states with the different inverse temperature β, i.e. with the different density. Bumper-to-bumper distance r_i among the

succeeding cars (ith and $(i-1)$th) is calculated (after eliminating car-truck, truck-car, and truck-truck gaps) via standard formula

$$r_i = v_i(t_i - t_{i-1}),$$

by means of netto time-headway $t_i - t_{i-1}$ and velocity v_i of ith car (both directly measured with induction-loop detector) supposing that velocity v_i remains constant between the times t_i, t_{i-1} when ith car and the previous one are passing a measure point. Such a condition could be questionable, especially in the region of small densities where the temporal gaps are too large. However, the influence of a possible error is of marginal importance, as apparent from the fact, that distribution function plotted for small-density data do not show any visible deviation from Poisson behavior expected for independent events (see Fig. 4 and relation (15)).

We note that mean distance among the cars is re-scaled to one in all density-regions. The thorough statistical analysis of the traffic data leads afterwards to the excellent agreement between clearance distribution computed from traffic data and formula (14) for fitted value of inverse temperature β_{fit} (see Fig. 4). We have obtained the fit parameter β_{fit} by a least-square method, i.e. minimizing the error function χ^2. The deviation χ^2 between the theoretical and empirical clearance distributions is plotted in Fig. 5 (low part).

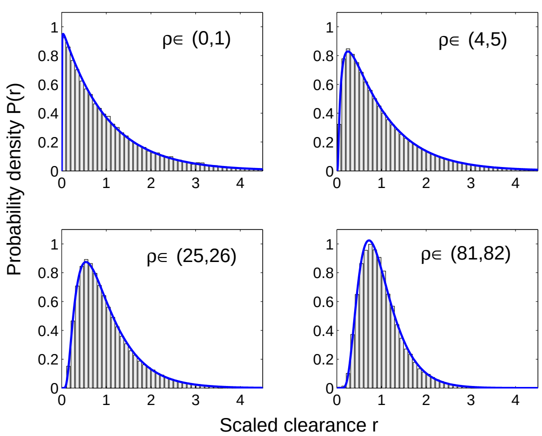

Figure 4. Probability density $P(r)$ for scaled spacing r between successive cars in traffic flow.
Histograms represent the clearance distributions computed for traffic data from indicated density region (in $\mathrm{veh/km/lane}$). Note that mean distance among the cars is re-scaled to one in all density-regions. The curves represent the predictions of statistical model (14) for fitted value of inverse temperature β_{fit}. The respective values β_{fit} were carefully analyzed and consecutively visualized in the following Fig. 5 (top part).

Dimensionless inverse temperature β of the traffic sample, representing a quantitative description of mental strain under which the car-drivers are in a given situation, shows non-trivial dependence on traffic density ϱ (as visible in Fig. 5 – top part). For free flow states ($\varrho \lesssim 20\ \mathrm{veh/km/lane}$) one can recognize a rise in temperature having a linear behavior (up to $10\ \mathrm{veh/km/lane}$) and visible plateau above. In the intermediate region (between 20 and $50\ \mathrm{veh/km/lane}$), where free traffic converts to the congested traffic, we detect a sharp increase in the first half. Such a behavior can be simply elucidated by the fact that the drivers, moving quite fast in a relatively dense traffic flow, are under a substantial psychological pressure, which finally results (for densities $\varrho \in [35, 50]\ \mathrm{veh/km/lane}$) in the transition to the congested flows a therefore in the drop in inverse temperature. In synchronized traffic regime ($\varrho \gtrsim 50\ \mathrm{veh/km/lane}$) the drivers vigilance rapidly grows up which culminates by the traffic-jam formation.

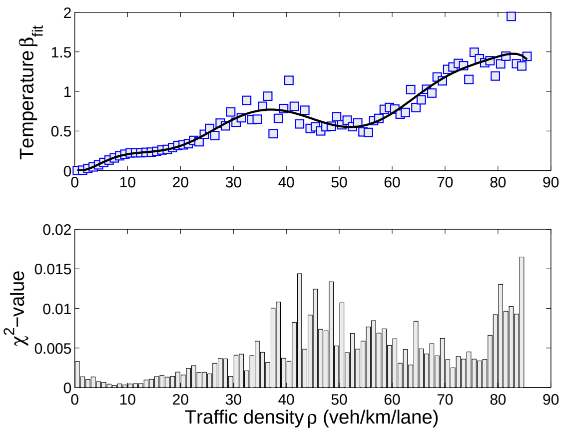

Figure 5. Inverse temperature β_{fit} and deviation χ^2 as a function of traffic density ϱ.
Squares stand for values of fit parameter β_{fit}, for which the function (14) coincides with clearance distribution of traffic data. The curve represents a polynomial fit of relevant data. Bars from lower part correspond to the sums of squared deviations between the empirical and the theoretical netto distance distributions for β_{fit}. We note that the value of normalization constant B was determined via formula (8), because the values of relevant inverse temperatures lie in interval $[0, 2]$, where the linear approximation (10) is less suitable (see deviations in Fig. 2). Second normalization constant A was calculated by means of equation (9).

For completeness we have compared real-road clearance distributions with probability density (5) specified for power-law potentials $V(r) = r^{-\alpha}$, where $\alpha = 2, 3, 4, 5$, respectively. Similar analysis was already introduced in article [7]. As results from the careful analysis of statistical deviations χ^2, relevant distributions (5) – obtained by applying a least-square method – predicate the inter-vehicle gaps substantially worse than those calculated for $\alpha = 1$ (follow Fig. 6). We emphasize that small deviations χ^2 (indicating a good agreement) detected near the origin in Fig. 6 are caused by the fact that for low traffic-densities the interactions among the cars are vanishing and inter-vehicle gaps are therefore practically independent. The relevant distributions in this case came close to the Poisson distribution (see upper left-hand subplot of Fig. 4). However, the Poisson distribution can be obtained as a limit of distribution (3), i.e.

$$\lim_{\beta \to 0_+} P_\beta(r) = e^{-r}, \tag{15}$$

for arbitrary function $V(r)$. For that reason it is impossible to detect the interaction potential in traffic sample using the low density data only. The comparison of various potentials $V(r) = r^{-\alpha}$ (including the logarithmical potential $V(r) = -\ln(r)$) brings finally the message that interaction among the vehicles in traffic stream can be very well

estimated by the short-ranged two-body power-law potential $V(r) = r^{-1}$. Predicted inter-vehicle-gap distributions correspond in this case to the computed probability density in all density intervals.

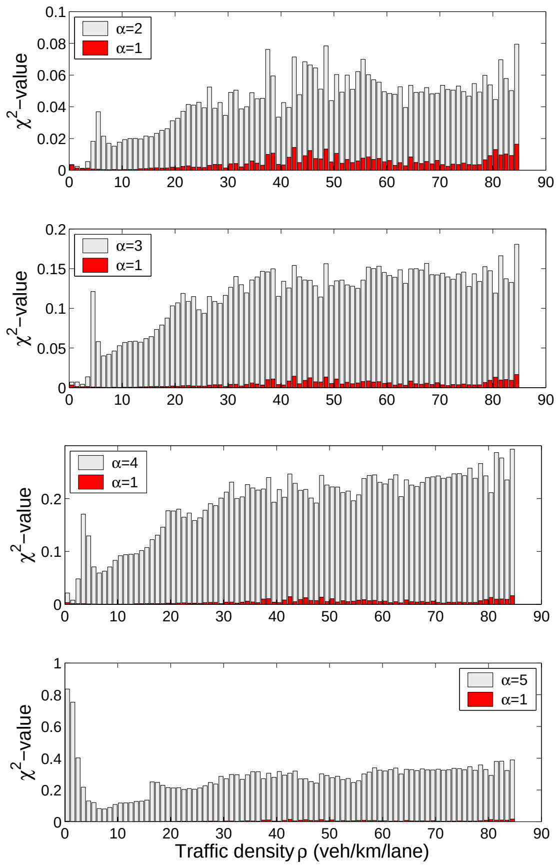

Figure 6. Deviation χ^2 between clearance distribution of cars moving in traffic stream and normalized distribution (5) evaluated for $\alpha = 2, 3, 4, 5$, respectively.
Grey bars represent the sums of squared deviations depending on traffic density for $\alpha = 2, 3, 4, 5$, respectively. Dark bars display the relevant deviations for $\alpha = 1$ previously plotted in Fig. 5 (lower part).

We append that another suitable quantity for comparison with single-vehicle data is a time-clearance distribution as well. Furthermore, time gaps among the succeeding cars are directly measurable and therefore not burden with errors caused by computation approximations. Determination of exact form for time-headway probability density of above thermodynamical traffic gas and relevant comparison with highway traffic data will be incorporated in the continuing work. Nevertheless, several analytical forms for corresponding distribution have already been discussed in article [5] and also in book [10].

To conclude we have found the analytical form of the thermal-equilibrium spacing distribution for one-dimensional traffic gas which neighboring particles are repulsed by the two-body potential $V = r^{-\alpha}$, where r is their mutual distance. The values of two normalization constants were successfully estimated by the convenient approximations. The calculated distribution (for $\alpha = 1$) with one free parameter (inverse temperature β) has been compared to the distance clearance distribution of the freeway traffic samples with the excellent outcome. It was demonstrated that inverse temperature of traffic sample non-trivially depends on the traffic density. The obtained agreement between experimental and calculated distributions confirms a convenience of the traffic potential used for description of local traffic interactions. Presented article crowns the quest for the mathematical formula for probability density of mutual clearances among the cars in traffic stream and supports the possibility for applying the equilibrium statistical physics to the traffic modelling.

Acknowledgements: We would like to thank Dutch Ministry of Transport for providing the single-vehicle induction-loop-detector data. This work was supported by the Ministry of Education, Youth and Sports of the Czech Republic within the project LC06002.

References

[1] E.B. Bogomolny, U. Gerland, and C. Schmit, Eur. Phys. J. B **19** (2001), 121

[2] D. Helbing, Rev. Mod. Phys. **73** (2001), 1067

[3] D. Helbing and M. Treiber, preprint: cond-mat/0307219

[4] D. Helbing and M. Treiber, Phys. Rev. Lett. **81** (1998), 3042

[5] D. Helbing, M. Treiber, and A. Kesting, Physica A **363** (2006), 62

[6] L. Neubert, L. Santen, A. Schadschneider, and M. Schreckenberg, Phys. Rev. E **60** (1999), 6480

[7] M. Krbalek and D. Helbing, Physica A **333** (2004), 370

[8] M. Krbalek, P. Seba, and P. Wagner, Phys. Rev. E **64** (2001), 066119

[9] R. Mahnke, J. Hinkel, J. Kaupužs, and H. Weber, preprint: cond-mat/0606509

[10] A.D. May, *Traffic flow fundamentals*, Prentise Hall, Englewood Cliffs, New Jersey, 1990

[11] R. Scharf and F.M. Izrailev, J. Phys. A: Math. Gen. **23** (1990), 963